Bioorganic & Medicinal Chemistry 16 (2008) 9871–9881

Contents lists available at ScienceDirect

Bioorganic & Medicinal Chemistry

journal homepage: www.elsevier.com/locate/bmc

Interactions of sodium and potassium ions with oligonucleotides carrying human telomeric sequence and pyrene moieties at both termini

Hirohisa Hayashida [a], Jan Paczesny [b], Bernard Juskowiak [b], Shigeori Takenaka [a,*]

[a] Department of Applied Chemistry, Faculty of Engineering, Kyushu Institute of Technology, Kitakyushu-shi 804-8550, Japan
[b] Faculty of Chemistry, A. Mickiewicz University, Poznan, Poland

ARTICLE INFO

Article history:
Received 15 April 2008
Revised 9 August 2008
Accepted 14 August 2008
Available online 26 August 2008

Keywords:
G-quadruplex
Human telomere sequence
Fluorescent probe
Potassium ion
Potassium sensing oligonucleotide
Hybrid-type quadruplex
Pyrene tag
Anisotropy
Circular dichroism
Native PAGE

ABSTRACT

The organization of human telomeric DNA is of intense interest because of its role in aging, cancer research and bioanalytical applications. The Htelom sequence 5′-$G_3(T_2AG_3)_3$-3′ has been use to prepare two pyrene-modified fluorescence probes with three- and six-carbon linkers: Py-Htelom-Py(C3) and Py-Htelom-Py(C6), respectively. Results of the circular dichroism (CD), native PAGE, steady-state fluorescence, and anisotropy measurements of sodium and potassium quadruplex formation by these pyrene-modified conjugates are presented and discussed in order to clarify which conformation facilitates or renders the pyrene/pyrene or G-tetrad/pyrene stacking interaction. The CD spectra and native PAGE images suggested that conjugation of pyrene moieties has negligible effect on the folding properties of Htelom oligonucleotide. CD melting profiles and thermodynamic parameters revealed that both sodium and potassium quadruplexes are stabilized by the anchoring of pyrene tags with potassium ion being more effective than its sodium counterpart. Monomer emission of pyrene dominated in all investigated systems with fluorescence intensity being sensitive to the nature and concentration of cation and this phenomenon was attributed to the quenching processes and to the particular topologies of sodium and potassium quadruplexes. Strong quenching observed in the presence of KCl was attributed to the peculiarity of the potassium hybrid-type quadruplex, which enables effective stacking of pyrene moieties on the exposed guanine tetrads, thus facilitating static or electron transfer quenching. Plausibility of stacking interactions between pyrene and G-tetrad in a hybrid-type potassium quadruplex was further supported by the anisotropy measurements and molecular modeling results.

1. Introduction

Certain DNA sequences that are guanine rich can form four-stranded structures called quadruplexes under specific cation conditions.[1–4] These structures have been identified in chromosome ends,[5] thrombin-binding aptamer,[6] and also in the promoter region of certain oncogenes, such as c-MYC and BCL2.[7–9]

In vitro characterization of quadruplexes indicates four-stranded structures containing one or more nucleic acid strands, in parallel or antiparallel orientations, stabilized by coordination of a monovalent cation within its central channel[10,11]. Four guanines on a plane interacting via Hoogsteen bonding form a G-quartet (Fig. 1a). Typically, three or four G-quartets are stacked and held together by π–π nonbonded attractive interactions, but formed quadruplexes may have different topological structures as shown in Figure 1b–e.

Oligonucleotide with human telomere sequence [$G_3(T_2AG_3)_3$] denoted here as Htelom is the most frequently investigated because its quadruplex is regarded as a target for inhibiting telomerase activity and as a complexing moiety in fluorescent probe for detecting potassium concentration under physiological conditions (PSO—potassium sensing oligonucleotide).[12–16] The fluorescent K^+ sensor developed by us, exploited fluorescence resonance energy transfer (FRET) as a transduction process. The PSO has been recommended for the monitoring of K^+ in an excess of Na^+. However, the FRET sensors appeared to exhibit more complex response that could be explained by FRET exclusively. For example, higher FRET signal was observed for the PSO/Na^+ complex, which suggested stacking interactions of fluorophores and quenching in the K^+-quadruplex but these peculiarities were not further studied.[14,16] Our next fluorescent probe denoted as PSO-py, exploited the 15-meric thrombin-binding aptamer (TBA) with a d(GGTTGGTGTGGTTGG) sequence as a cation-binding moiety and the pyrene excimer emission for the transduction of the cation-binding event.[17] Contrary to the FRET approach, stacking interactions between fluorophores (pyrenes) were advantageous for excimer formation and efficient excimer emission was indeed observed for the PSO-py/K^+ complex, while the random coil structure of PSO-py in the absence of K^+ gave only monomer emission.[17] Excimer emission was attributed to a chair-type

* Corresponding author. Tel./fax: +81 93 884 3322.
E-mail address: shige@che.kyutech.ac.jp (S. Takenaka).

0968-0896/$ - see front matter © 2008 Elsevier Ltd. All rights reserved.
doi:10.1016/j.bmc.2008.08.035

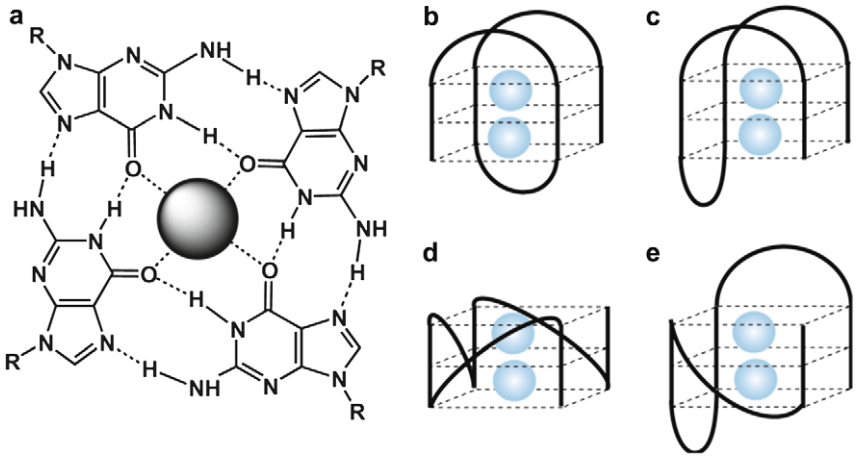

Figure 1. Structures of G-tetrad (a) and the four types of intramolecular G-quadruplexes: antiparallel basket-type (b) and chair-type (c), parallel propeller-type (d), and hybrid mixed-type (e). Encapsulated metal cations are shown as balls.

topology of the PSO-py/potassium quadruplex, in which both 3′- and 5′-termini of TBA possess adjacent orientation, thus facilitating face-to-face alignment of pyrene tags. On the other hand, the FRET-based sensor containing TBA oligonucleotide and a FAM/TAMRA donor/acceptor pair was reported to produce rather poor FRET signal that was explained by quenching of TAMRA fluorescence due to the dye–dye interactions with FAM.[18] It should be pointed out that TBA is known to form only single, a chair-type quadruplex irrespectively to the metal cation complexed.[6] Contrary to TBA oligonucleotide, the human telomere repeat sequence is suspected to coexist in several structures in the presence of potassium ion (Fig. 1b–e): a chair- and a basket-type, a propeller-type or a hybrid-type and the problem of the interconversion of particular structures is still under debate.[19–26] For further rational design and development of quadruplex-based fluorescent sensing devices it is very important to clarify, which quadruplex conformation facilitates or renders the fluorophor/fluorophor or G-tetrad/fluorophore stacking interactions.

For this purpose, we designed and synthesized Py-Htelom-Py oligonucleotide probes, carrying human telomeric sequence and pyrene moieties at its termini. Two fluorescent probes were synthesized (Scheme 1); one, abbreviated as Py-Htelom-Py(C3), with pyrenes linked to oligonucleotide by three-carbon spacers, and second, Py-Htelom-Py(C6), with six-carbon linkers.

We expected that these oligonucleotides should exhibit sensitivity of monomer/excimer emission intensities to the particular topological structure of tetraplex. As depicted in Figure 2, a basket-type quadruplex (sodium complex) should emit mainly monomer emission because of steric hindrance imposed by a diagonal TTA loop that prevent Py–Py interactions and formation of excimer, but a chair-type quadruplex is expected to show efficient excimer emission, similarly as it was observed for TBA probe with the same chair-like conformation.[17] Two other structures, propeller and hybrid quadruplexes, may show both monomer or excimer emission depending on the conformation of pyrene tags, which prevent or allow the formation of a sandwich-type excimer structure (type B arrangement). Moreover, pyrene rings may also stack on the external G-tetrad, which should cause strong quenching effect (type A arrangement). Peculiarity of a quadruplex (propeller vs hybrid structure) and length of a spacer (C3 or C6) may affect perfect formation of the sandwich-type pyrene dimer or stacking with G-tetrads, thus the probes may exhibit different spectral characteristics. Results of the circular dichroism (CD), steady-state fluorescence and anisotropy measurements of sodium and potassium

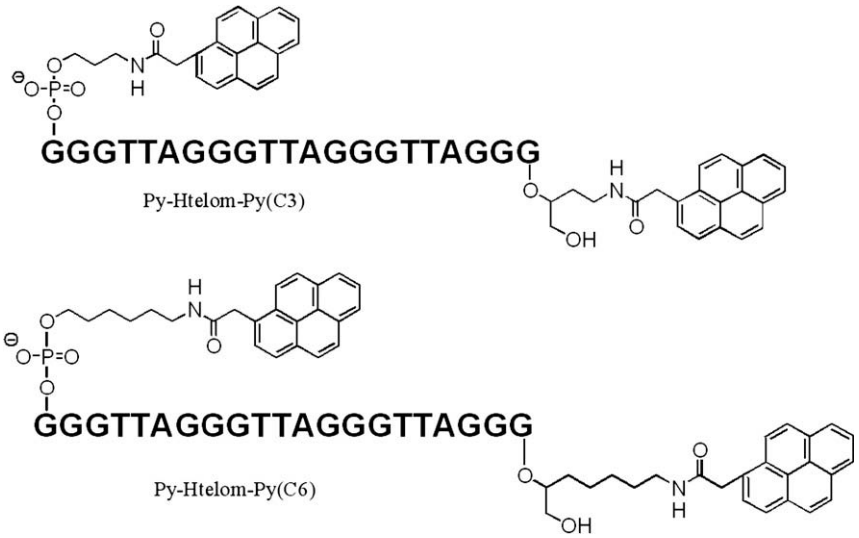

Scheme 1.

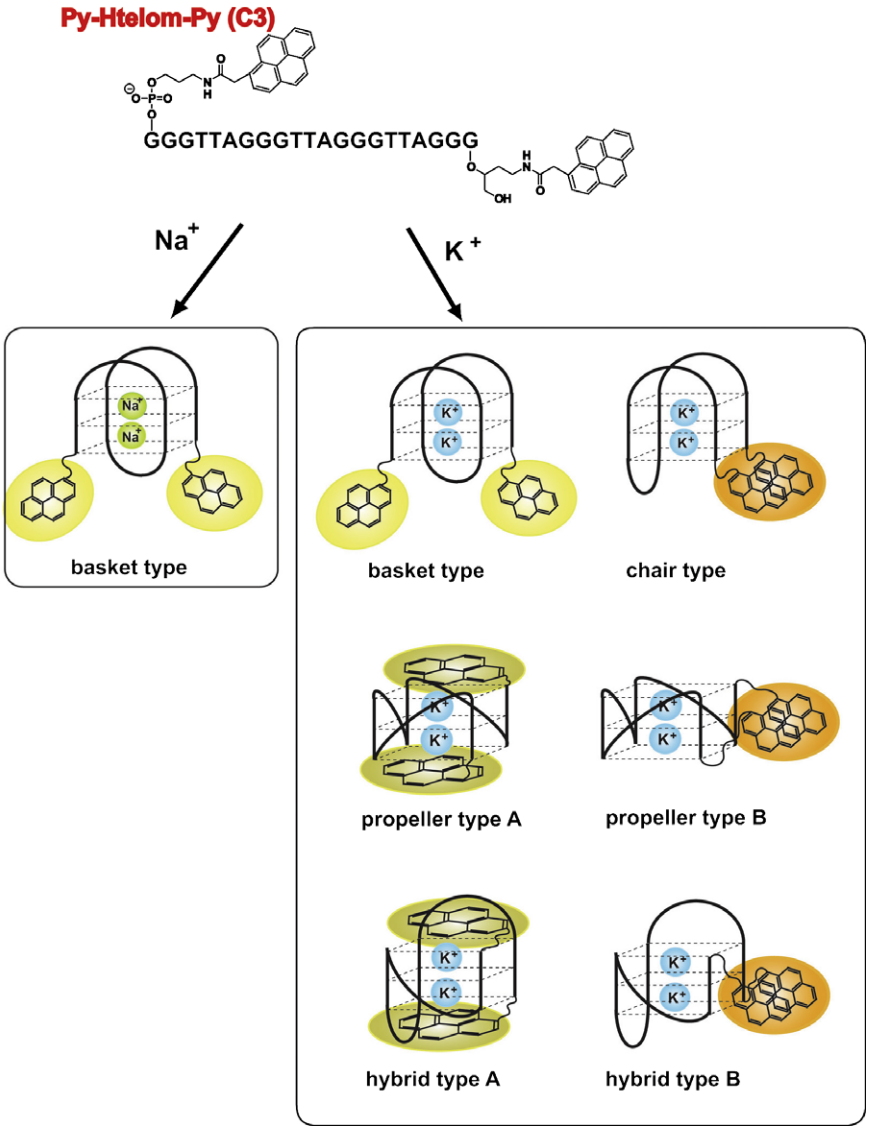

Figure 2. Expected tetraplex structures of Py-Htelom-Py probes showing pyrene tags arrangements in the presence of sodium or potassium ion.

quadruplexes formed by the pyrene-modified oligonucleotides with human telomeric sequence, are presented and discussed here.

2. Results and discussion

2.1. Quadruplex formation by Py-Htelom-Py probes proved with CD spectroscopy, native PAGE electrophoresis and melting study

Incorporation of two pyrene labels can affect folding ability of the modified oligonucleotide, therefore, it is very important to examine the quadruplex formation process using alternative techniques, for example, gel electrophoresis and CD titration experiments.

The electropherograms of Py-Htelom-Py oligonucleotides in nondenaturing polyacrylamide gel containing 100 mM NaCl (Fig. 3a) or KCl (Fig. 3b) confirm that the pyrene-modified Htelom oligonucleotides, Py-Htelom-Py(C3) and Py-Htelom-Py(C6), migrate faster than the single stranded 20-mer DNA in accordance with the mobility of a intramolecular folded quadruplex formed by the unmodified [$G_3(T_2AG_3)_3$] Htelom oligonucleotide.[26] These PAGE images disprove the existence of unfolded probes or formation of multistranded structures.

More detail studies on G-quadruplex formation with pyrene-conjugates were carried out using CD spectroscopy.

The CD spectra of Py-Htelom-Py probes in Tris–HCl buffer titrated with NaCl are shown in Figure 4. Weak CD peaks are observed for both probes in the absence of NaCl, whereas addition of salt causes an appearance of the positive bands at 295 and 245 nm and negative band at 270 nm characteristic of the antiparallel quadruplex with a basket-type structure containing two lateral and one diagonal TTA loops.[19] The intensity of the CD bands rises as the salt concentration increases up to 10 mM NaCl (Fig. 4c). Further addition of salt causes only minor effect on the CD spectra of both probes, indicating that 10 mM concentration of NaCl is sufficient for nearly complete formation of quadruplex. The slightly higher intensity of CD bands for Py-Htelom-Py(C3) probe comparing to those for Py-Htelom-Py(C6) conjugate may indicate that six-carbon linker is less favorable for the formation of a perfect Na/Htelom quadruplex.

The variations in CD spectra of pyrene-modified oligonucleotides induced by the binding of potassium ion are shown in Figure 5. Interestingly, one can observe difference in the pattern of CD spectra for both probes in the absence of salt that may be caused by the effect of linker length (three vs six carbons). The

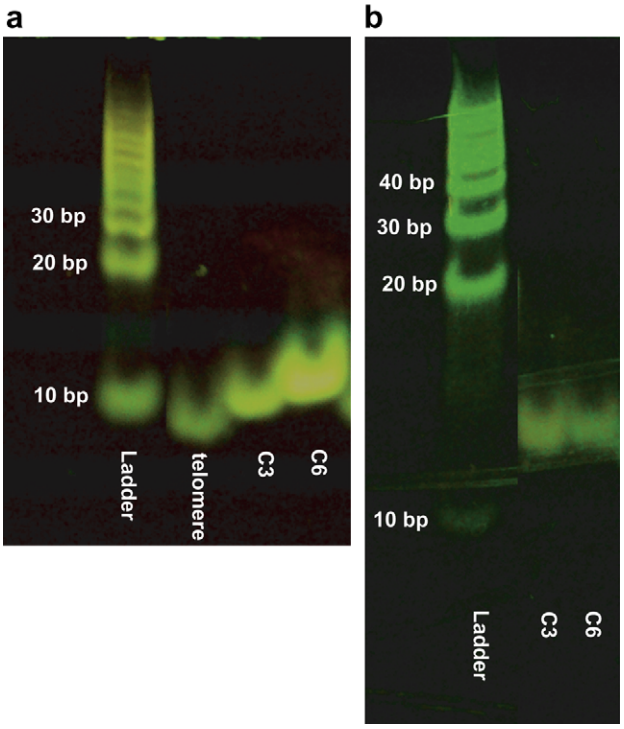

Figure 3. Native PAGE images of unmodified Htelom oligonucleotide $G_3(T_2AG_3)_3$ (telomere) and pyrene-modified Htelom oligonucleotides (C3 and C6 denote Py-Htelom-Py(C3) and Py-Htelom-Py(C6) probes, respectively) in 20 mM Tris–HCl buffer (pH 7.4) containing 0.1 M NaCl (a) and 0.1 M KCl (b).

presence of a modest positive peak at 260 nm (Fig. 5b), which is indicative of a parallel structure,[23,28] may suggest that C6 linker facilitates partial self-folding of the probe into a propeller-type assembly in the absence of metal ion. However, subsequent additions of KCl resulted in the development of a large positive band at 290 nm for both ligands that is consistent with the literature data concerning CD spectra of K/Htelom quadruplex.[23–28] The saturation plots in Figure 5c show that both oligonucleotides reached their final tetraplex structures at 1 mM KCl. According to most recently published reports, a mixed-type hybrid quadruplex (Fig. 1e) dominates in KCl solution of Htelom oligonucleotide, but its fractional contribution depends on the length of oligonucleotide,[23,24] modification of guanine[25] and the presence of crowding agents in solution (e.g., polyethylene glycol).[21] Problem of structural polymorphism of Htelom/K^+ complex is still under debate since other structures, which may contribute to the overall CD spectrum of a mixture, possess similar CD spectra (a chair- and a basket-type quadruplexes). Another possible structure that may coexist in aqueous KCl solution was reported by Parkinson et al. for a solid-state potassium complex.[3] This propeller-like quadruplex features a parallel orientation of strands with double-chain-reversal side loops (Fig. 1d).[3] This structure was also observed in solution by NMR for a modified two-repeat Htelom sequence.[29] However, the CD spectra reported for most Htelom sequences in KCl solution (e.g., Fig. 5) are radically different from the CD spectrum of a parallel structure, which possesses a strong positive band at 260 nm.[25,28–30] Therefore, the parallel structures may be present in investigated systems only as a minor component.[20,21] The existence of hybrid quadruplex as a major component in investigated systems seems to be justified in light of literature data including peculiar CD spectra.[22–25] This mixed-type hybrid quadruplex contains two lateral loops and one external loop (Fig. 1e), which give mixed parallel–antiparallel orientation of strands with a characteristic CD spectrum showing a strong positive band at 290 nm, with weak negative peaks around 235–255 nm.

Concluding, although there are some differences in overall shapes of CD bands (especially in the absence of metal ion), the final CD spectra of metal complexes are consistent with the literature data for unmodified Htelom oligonucleotide,[23–28] which means that conjugation of pyrene moieties has negligible effect on the folding properties of Htelom oligonucleotide.

Thermal stability of the tetraplex structures of the pyrene-modified oligonucleotides was evaluated in the presence of KCl or NaCl using the temperature dependence of CD spectra. The obtained melting profiles are shown in Figure 6. One should note an increase in molar ellipticity for K/Htelom-Py systems (Fig. 6a) at the beginning of melting plots (20–40 °C), which can be associated with formation of more perfect quadruplex structure. One can expect that stabilizing effect of two stacked pyrenes or a pyrene interacting with the terminal G-tetrad may result in distortion of the guanine alignment in a quadruplex. Consequently, an increase in temperature weakens the stacking interactions leading to more perfect guanine arrangement and an increase in molar ellipticity as observed in Figure 6a. The lack of such a phenomenon for sodium quadruplexes (Fig. 6b) suggests that quadruplex structure (hybrid- vs basket-type) plays an important role in this phenomenon to occur.

Effect of covalent attachment of the pyrene on the stability of particular quadruplexes can be compared through the thermodynamic parameters listed in Table 1. A parent oligonucleotide, Htelom, provides a reference since the thermodynamic parameters for Na/Htelom and K/Htelom complexes are in good agreement with previous studies.[27,31,32] Sodium quadruplexes are slightly stabilized by the attachment of pyrene (ΔT_m = 4–5 °C), whereas in case of K/Py-Htelom-Py(C3) and K/Py-Htelom-Py(C6) quadruplexes this effect is substantial with ΔT_m approaching 13 and 15 °C, respectively. Thermal stabilization of pyrene-modified oligonucleotide has been also reported for molecular beacon with a stem–loop structure and this effect was ascribed to the pyrene–pyrene hydrophobic or π–π interactions.[33] On the other hand, Mergny et al. reported that modification of Htelom oligonucleotide with FRET labels, fluorescein and tetramethylrhodamine, destabilized quadruplex structure, which was accounted for the presence of a negatively charge on the conjugated fluorescein dye.[32]

Inspection of thermodynamic data collected in Table 1 reveals that both sodium and potassium quadruplexes are stabilized by the anchoring pyrene functions with potassium ion being more effective than its sodium counterpart. Since the ΔH changes for conjugates are less favorable when compared with those for unmodified oligonucleotides, it is evident that the contribution for the higher stability of covalently modified probes is entropic in origin. The dangling hydrophobic pyrene moieties in the unfolded state of Htelom probe possess hydration shell, which is released upon folding into a quadruplex. This may suggest that pyrene moieties are stacked on the terminal guanine tetrads in a quadruplex since pyrene–pyrene sandwich interactions are less plausible (no excimer emission observed—vide infra).

2.2. Fluorescence of pyrene-modified oligonucleotides and anisotropy studies

The various hybridization studies on oligonucleotides possessing pendent pyrene chromophores have established that the proximity of two pyrenes is a necessary, but not sufficient condition for the excimer fluorescence to occur. Conformations, which do not allow the formation of a sandwich face-to-face excimer structure for the electronically excited pyrene dimer, give rise to monomer or broadened monomer fluorescence rather than excimer emis-

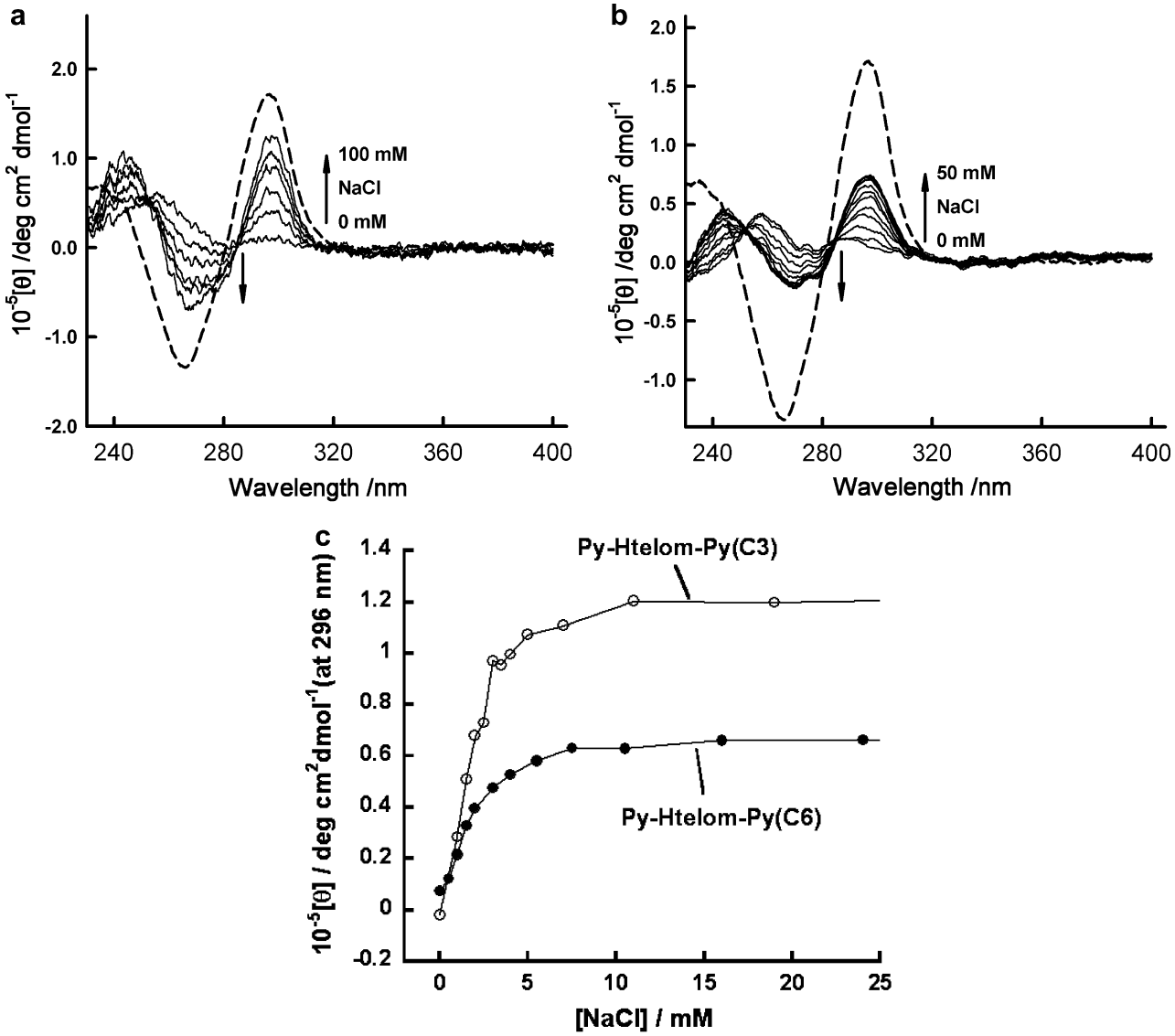

Figure 4. CD spectra of 2 μM Py-Htelom-Py(C3) (a) and 1.8 μM Py-Htelom-Py(C6) (b) recorded upon addition of NaCl in 20 mM Tris–HCl buffer (pH 7.4). A spectrum of unmodified Htelom oligonucleotide in the presence of 100 mM NaCl is included (broken line). (c) Molar ellipticities of the CD band at 296 nm were plotted against the concentration of NaCl.

sion.[33–38] Figure 7 shows the fluorescence spectra of pyrene-modified oligonucleotides recorded in the presence of varied amount of NaCl. A typical emission characteristic of monomer pyrene with slightly broadened vibrational bands is observed. No excimer emission is visible in the 450–550 nm range that is not a surprise since a diagonal TTA loop in basket-type quadruplex separates two pyrenes effectively, preventing from excimer formation. The effect of NaCl concentration on pyrene emission is not straightforward, however: an increase in the concentration of NaCl results initially in a fluorescence enhancement followed by a quenching effect at NaCl concentrations exceeding 10 mM as shown in Figure 7c.

These bimodal changes in fluorescence intensity induced by NaCl addition can be explained by vulnerability of pyrene moiety to participate in quenching processes (a static quenching or an electron transfer from adjacent thymine or guanine bases[39]) and by particular topology of a basket-type sodium quadruplex. If one assumes that Htelom probes can exist in the absence of metal ions or at low salt concentration as hairpin structures,[40,41] then pyrene emission may be partially quenched by neighboring G:G base-pair even in the absence of cations. Thus, initial enhancement of pyrene emission may be ascribed to the dequenching process since formation of basket-type-quadruplex may require disruption of such a preorganization of oligonucleotide. Similar dequenching processes and subsequent fluorescence enhancement have been reported for NaCl effect on a TAMRA-labeled Htelom oligonucleotide.[16] It should be noted that fluorescence increases up to 10 mM NaCl in good agreement with completion of the quadruplex formation process as shown by CD titration experiments (Fig. 4). However, further increase in NaCl concentrations leads to reappearance of the quenching phenomenon. Pyrene emission decreases gradually approaching finally a constant level at higher NaCl concentrations (Fig. 7c). The latter quenching may be caused by the same origin, that is, electron transfer (ET) to thymine in TTA diagonal loop or static process due to stacking interactions. Stacking interactions between hydrophobic pyrene rings and nucleobases are plausible at higher salt concentration due to the phenomenon known as electrostriction.[42]

Changes in fluorescence spectra of Py-Htelom-Py probes are more pronounced in the presence of KCl as shown in Figure 8. Dramatic quenching of monomer band is observed for Py-Htelom-

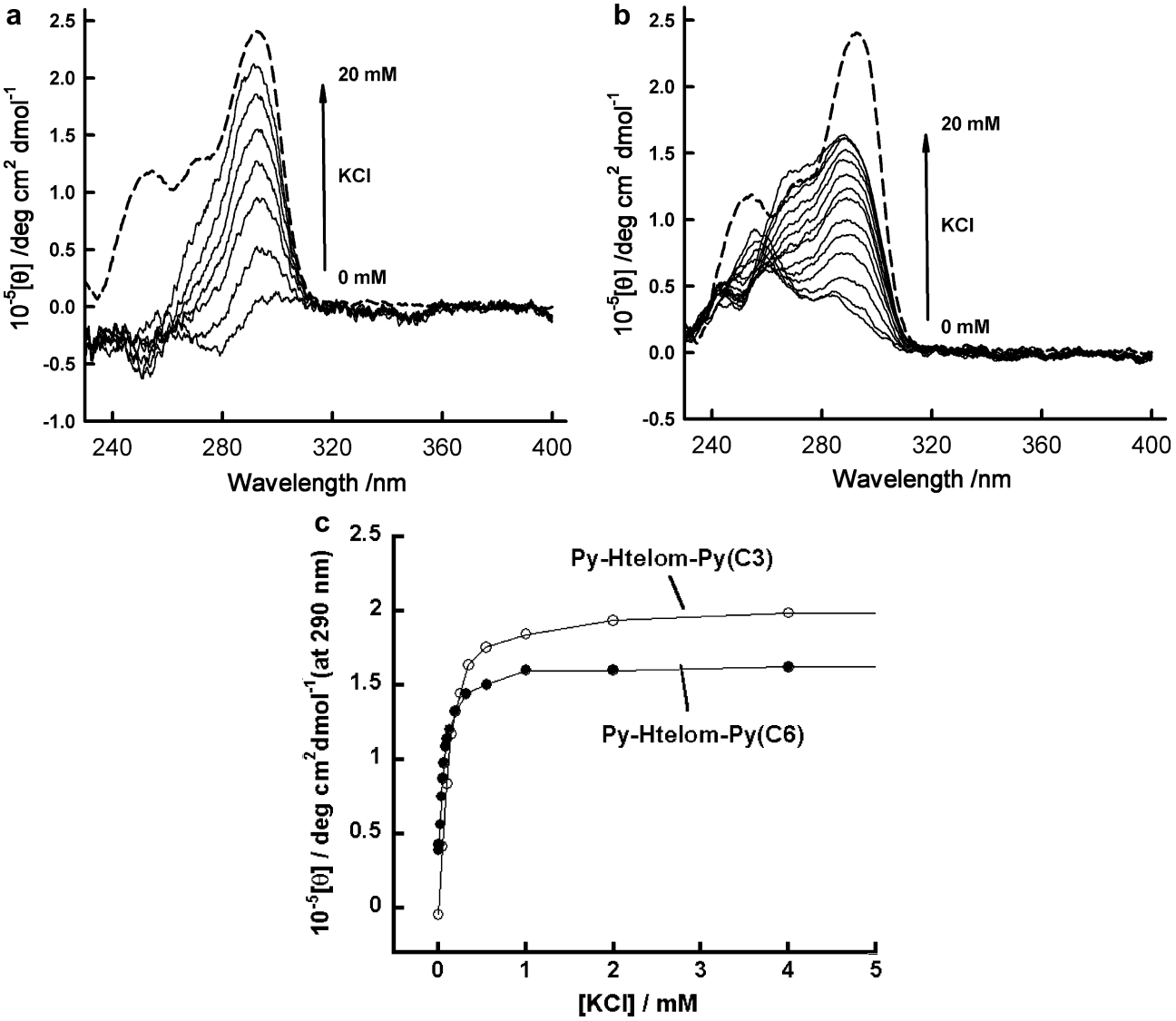

Figure 5. CD spectra of 2 μM Py-Htelom-Py(C3) (a) and 1.8 μM Py-Htelom-Py(C6) (b) recorded upon addition of KCl in 20 mM Tris–HCl buffer (pH 7.4). A spectrum of unmodified Htelom oligonucleotide in the presence of 20 mM KCl is included (broken line). (c) Molar ellipticities of the CD band at 290 nm were plotted against the concentration of KCl.

Py(C3) probe while fluorescence of Py-Htelom-Py(C6) is quenched less efficiently. Additionally, a weak broad emission band around 500 nm with isoemissive point at 460 nm has developed at higher KCl concentration for Py-Htelom-Py(C6) probe (Fig. 8b), which may indicate formation of residual excimer species. Final level of the fluorescence quenching in the presence of excess of KCl approaches 80% and 50% for Py-Htelom-Py(C3) and Py-Htelom-Py(C6), respectively. The quenching is almost completed in the KCl concentration range of 0–2 mM, in agreement with CD titration plots representing the formation of potassium quadruplex (Fig. 4c).

Different shapes of KCl quenching profiles when compared to NaCl effect reflect peculiarities in the structures of sodium and potassium quadruplexes. In contrast to sodium quadruplex, the lack of initial enhancement for KCl is evident, indicating that formation of potassium quadruplex proceeds without substantial rearrangement of preformed oligonucleotide structure. Alternative explanation may involve two competitive quenching processes: one associated with preorganization of a probe and a second, more efficient, due to the G-quartet/pyrene stacking. Formation of the potassium quadruplex results in more efficient quenching since strong stacking quenching substitutes the less efficient process. The final strong quenching should be linked to stacking interactions and/or dynamic quenching through electron transfer (ET). Two quadruplex structures, propeller and hybrid-type (Fig. 1a and e, respectively) can explain observed efficient quenching in the presence of KCl. However, CD spectra strongly suggested that hybrid-type quadruplex dominates in KCl solution. External guanine tetrads can be easily approached by any hydrophobic guest molecule with a proper planarity. Pyrene moiety can thus effectively stack on the guanine tetrads facilitating static or ET quenching. Thymine bases present in lateral loops of hybrid-type quadruplex can quench additionally the emission of pyrene.[39]

The question arises whether the weak excimer emission for K^+/Py-Htelom-Py(C6) originates from a small fraction of a chair-type quadruplex or from a propeller-type structure. To examine the spectral properties of the propeller-type quadruplex, additional CD and fluorescence measurements have been carried out for the system containing 150 mM KCl in the presence of a 'crowding' agent, 50% polyethylene glycol (PEG 200). High content of PEG in aqueous solution is known to promote formation of parallel quadruplexes by Htelom oligonucleotide in the presence of KCl.[21] CD spectra of potassium quadruplexes recorded in 50% PEG 200 shown

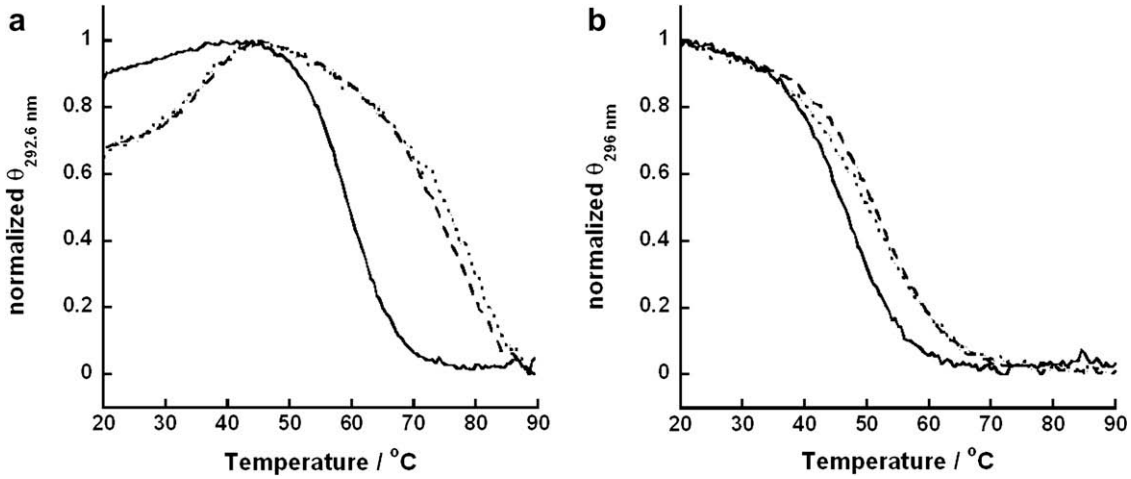

Figure 6. CD melting curves obtained in the presence of 20 mM KCl (a) and 20 mM NaCl (b). Solid line represents unmodified Htelom oligonucleotide, dashed line: Py-Htelom-Py(C3) probe, and dotted line: Py-Htelom-Py(C6) probe.

Table 1
The melting temperature (T_m) values and thermodynamic parameters of Htelom quadruplexes in the presence of 20 mM NaCl or 20 mM KCl

Quadruplex	T_m /°C	ΔH (kcal/mol)	ΔS (cal/mol K)	ΔG_{25} (kcal/mol)	ΔG_{37} (kcal/mol)
Na/Htelom [a)]	46.4 ± 0.6	−38.2 ± 1.6	−119.5±4.9	−2.57	−1.14
Na/Py-Htelom-Py(C3)	50.1 ± 0.7	−35.3 ± 0.9	−108.9±2.7	−2.82	−1.52
Na/Py-Htem-Py(C6)	50.5 ± 0.6	−30.8 ± 0.5	−95.3±1.5	−2.36	−1.24
K/Htelom [a)]	59.6 ± 0.5	−47.4 ± 5.5	−142.5±16.6	−4.91	−3.20
K/Py-Htelom-Py(C3)	72.5 ± 0.9	−42.5 ± 3.7	−123.0±10.6	−5.83	−4.35
K/Py-Htelom-Py(C6)	74.6 ± 1.1	−39.0 ± 3.2	−112.3±9.2	−5.76	−4.19

[a)] Htelom denotes human telomere sequence: $dG_3(T_2AG_3)_3$.

in Figure 9 exhibit for all probes (including unmodified Htelom oligonucleotide) a strong positive band at ca. 260 nm characteristic of a propeller-type structure.[26,28,30] Fluorescence spectra of these parallel quadruplexes (Fig 10) show only monomer emission of pyrene; moreover, addition of KCl results in fluorescence enhancement in contrast to aqueous solutions of investigated probes, in which fluorescence was quenched. The lack of excimer emission and the presence of fluorescence enhancement effect for propeller-type quadruplex may indicate that the occurrence of this structure in aqueous KCl solutions of pyrene-modified Htelom probes should be rather excluded. On the other hand, the obtained results should be treated with caution since the presence of 50% PEG may diminish stacking interactions between pyrene moieties, thus, may affect excimer formation. Therefore, we attempted to prove the ability of a parallel quadruplex to facilitate pyrene excimer emission using the Sr^{2+}/Htelom quadruplex, which was reported to exhibit CD spectrum characteristic of the parallel structure.[30,31] Unexpectedly, the CD spectra of Py-Htelom-Py(C3) and Py-Htelom-Py(C6) in the presence of $SrCl_2$ (1.5 mM) showed positive bands at 295 and 245 nm and negative band at 270 nm characteristic of the antiparallel quadruplex with a basket-type structure. The same spectra were obtained irrespective of the sample treatment (freshly prepared or thermally treated and incubated overnight) as suggested by others.[30,31] Most probably, the presence of two pyrene labels disturbed in the formation of a parallel structure, which was observed for unmodified Htelom oligonucleotide.[30,31] In accordance with CD results, the fluorescence spectra of Sr^{2+}/Htelom-Py systems showed only the monomer emission band and enhancement effect, resembling the fluorescence behavior of sodium quadruplexes with a basket-type structure. Thus, the conclusion that parallel quadruplex structure inhibits excimer emission remains somewhat speculative.

To further prove the possibility of stacking interactions between pyrene and guanine tetrad in the hybrid-type quadruplex, anisotropy measurements were carried out for pyrene probes. Figure 11 shows results of fluorescence anisotropy titrations of Py-Htelom-Py(C3) and Py-Htelom-Py(C6) with NaCl and KCl. The correlation between anisotropy changes and quadruplex formation is obvious.

Rather modest changes in anisotropy are observed for Na^+ quadruplexes (Fig. 11a) with profiles showing an initial decrease in anisotropy at low NaCl concentrations followed by stabilization ($r \leqslant 0.02$) at higher NaCl concentration. Titration of probes with KCl resulted in much more pronounced changes in anisotropy of pyrene emission as shown in Figure 11b. Both conjugates exhibit an increase in anisotropy upon KCl addition with Py-Htelom-Py(C3) probe being much more sensitive to KCl addition. Final values of anisotropy attained for Py-Htelom-Py(C3) and Py-Htelom-Py(C6) in the presence of an excess of KCl were 0.09 and 0.04, respectively. The courses of anisotropy plots are generally consistent with the runs of quenching profiles (Fig. 8c) and can be explained by the structural differences between sodium and potassium quadruplexes, which influence the extent of interactions between pyrene and nucleobases (guanine tetrad). The specific features of a hybrid-type potassium quadruplex, consisting in two exposed planes of guanine tetrads, are responsible for the KCl induced increase in anisotropy. Stacking interactions with tetrad planes result in restriction of rotational freedom of pyrene tags. The Py-Htelom-Py(C3) conjugate exhibits a more dramatic increase in anisotropy relative to Py-Htelom-Py(C6), which is consis-

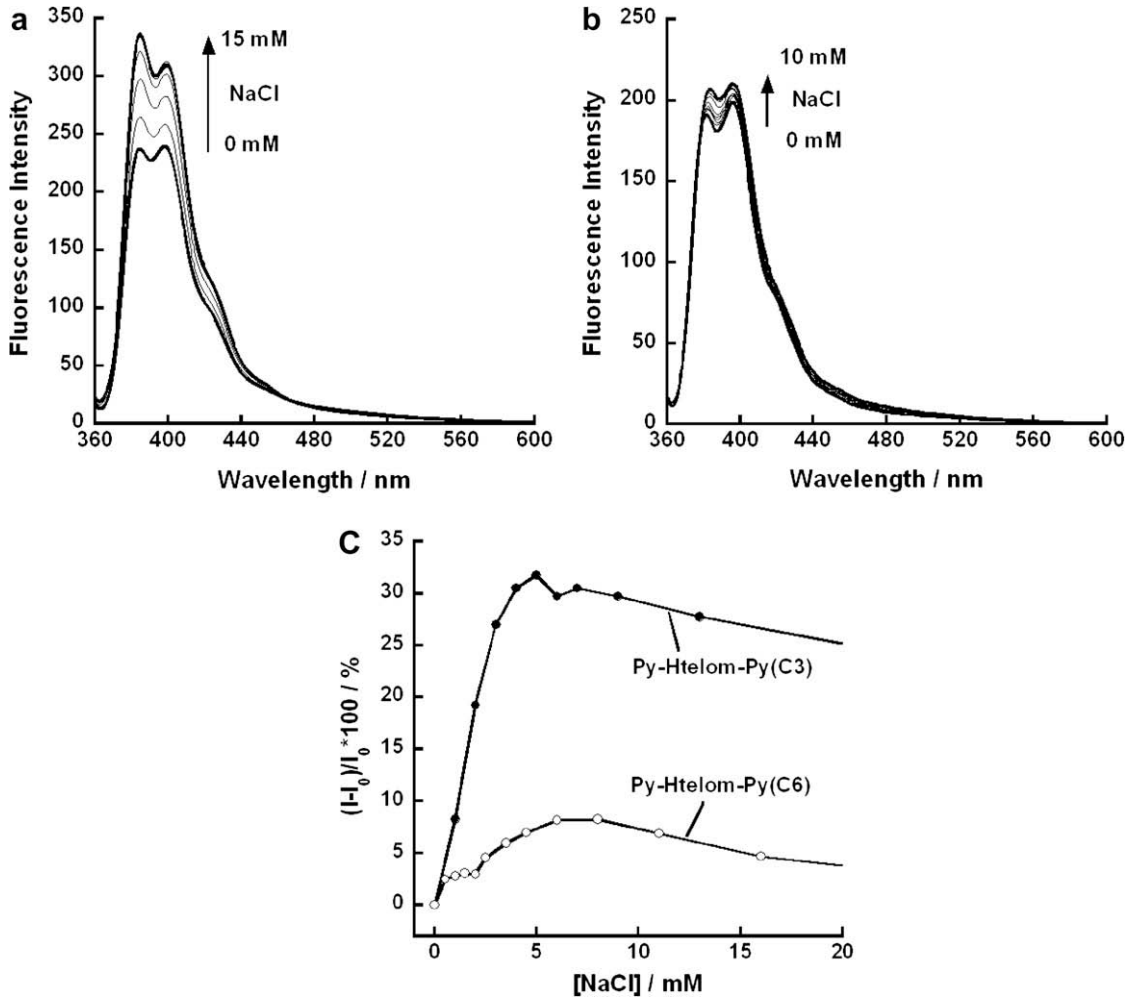

Figure 7. Fluorescence spectra of pyrene-modified oligonucleotides: (a) Py-Htelom-Py(C3) and (b) Py-Htelom-Py(C6) recorded upon titration with NaCl in 20 mM Tris–HCl buffer (pH 7.4). (c) Relative changes in fluorescence intensity (%) with the concentration of NaCl.

tent with more efficient quenching observed in the presence of KCl. Undoubtedly, different anisotropy levels attained for both probes reflect the extent of stacking interactions, which is a function of the rotational freedom of fluorophore moiety around a liker and the rotation and reorientations of the whole macromolecule.

Figure 12 shows optimized hybrid-type structures of potassium complexes, obtained with molecular modeling approach. Optimizations were performed with the Insight II package on a hybrid structure deposited in the Protein Data Bank under the accession code 2GKU and modified by removing terminal two thymines and one adenine from 5′- to 3′-ends, respectively. Pyrene moieties with respective linkers were next added to obtain Py-Htelom-Py(C3) and Py-Htelom-Py(C6) probes. As shown in Figure 12, both conjugates are able to form compact structures with pyrene moieties stacked on terminal guanine tetrads. The six-carbon linker in Py-Htelom-Py(C6) probe seems to impose some constrains preventing a perfect alignment of pyrene and the guanine tetrad (Fig. 12b), which is in good agreement with less efficient quenching of pyrene fluorescence (50% vs 80% for Py-Htelom-Py(C3)) and lower value of anisotropy of pyrene tag (0.04 vs 0.09 for Py-Htelom-Py(C3)). On the other hand, the residual excimer emission (Fig. 8b) may originate from a small fraction of quadruplexes with suitable ground state conformation of pyrenes enabling face-to-face dimer formation. Interconversion of a hybrid structure into a chair-type quadruplex as postulated by Sugiyama et al.,[25] may also explain residual excimer emission observed for KCl solution.

3. Conclusions

Results of the circular dichroism (CD), steady-state fluorescence and anisotropy measurements of sodium and potassium quadruplex formation by pyrene-modified oligonucleotides with human telomeric sequence, Py-Htelom-Py(C3) and Py-Htelom-Py(C6) were presented. The CD spectra and native PAGE experiments were generally consistent with the literature data for unmodified Htelom oligonucleotide, which suggested that conjugation of pyrene moieties have negligible effect on the folding properties of Htelom oligonucleotide. CD melting profiles and determined thermodynamic parameters revealed that both sodium and potassium quadruplexes are stabilized by the anchoring of pyrene tags with potassium ion being more effective than its sodium counterpart. For all investigated systems, only monomer pyrene emission was observed except for K^+/Py-Htelom-Py(C6) complex, which exhibited additional weak excimer emission at around 500 nm. Fluorescence intensity of pyrene monomer emission was sensitive to the nature and concentration of metal cations and this phenomenon was explained by the quenching processes (a static quenching or an electron transfer from adjacent thymine or guanine bases). On the other hand, the diverse quenching effect should be attributed to the structural differences between sodium and potassium quadruplexes and to the length of a linker (C3 vs C6). Moderate quenching effect and a lack of excimer emission was observed for sodium ion, which is known to form a basket-type quadruplex. The TTA

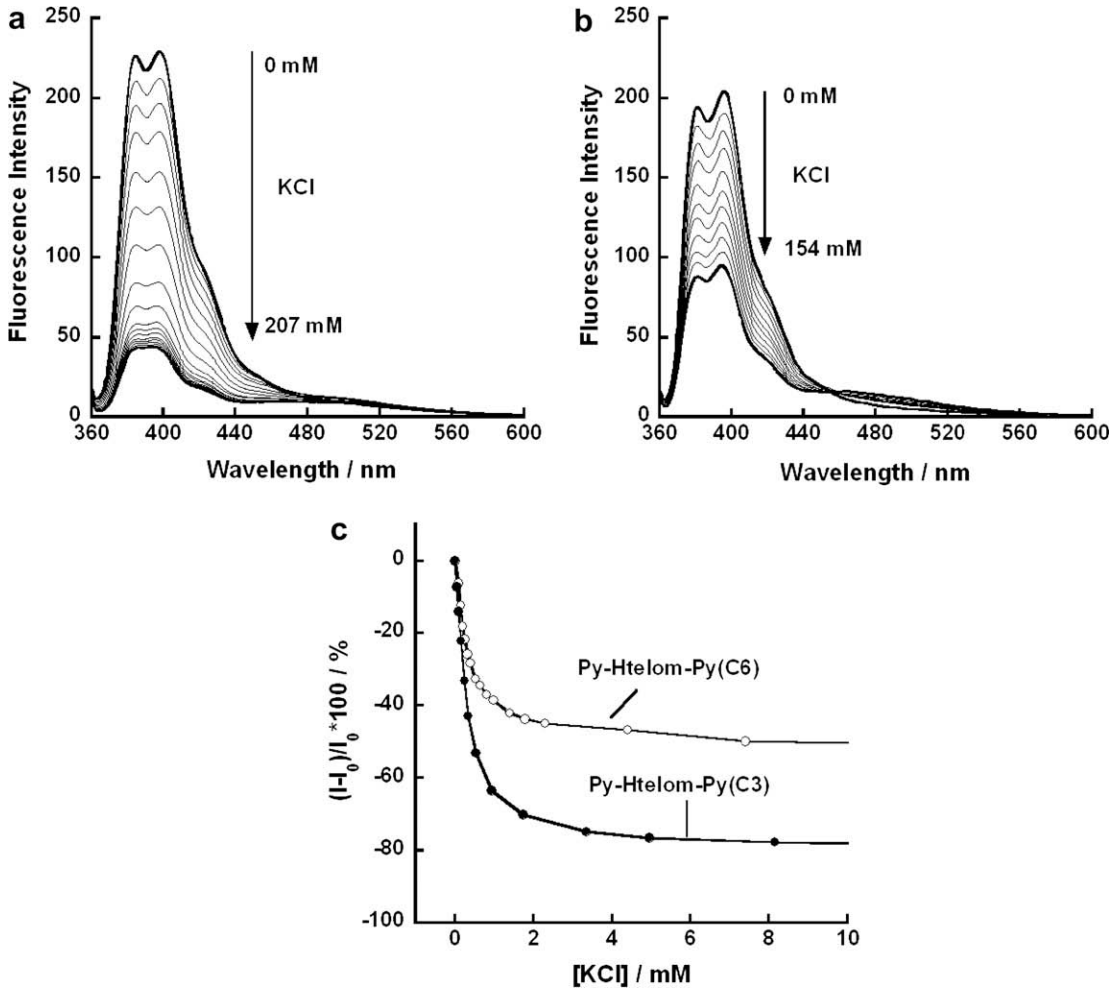

Figure 8. Fluorescence spectra of pyrene-modified oligonucleotides: (a) Py-Htelom-Py(C3) and (b) Py-Htelom-Py(C6) recorded upon titration with KCl in 20 mM Tris–HCl buffer (pH 7.4). (c) Relative changes in fluorescence intensity (%) with the concentration of KCl (λ_{ex} = 344 nm, λ_{em} = 398 nm).

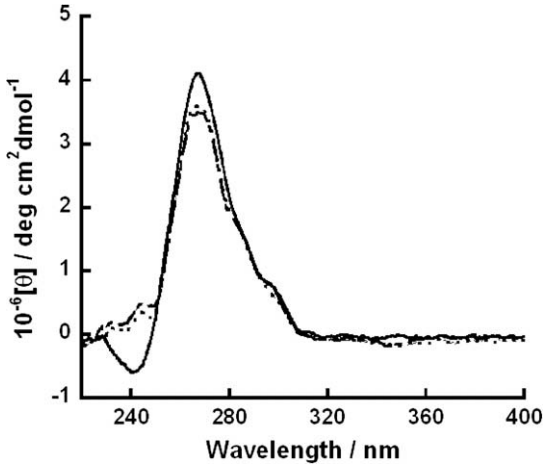

Figure 9. CD spectra of 2 μM Htelom (solid line), 2 μM Py-Htelom-Py(C3) (dashed line), and 2 μM Py-Htelom-Py(C6) (dotted line) recorded in the presence of 50% PEG200. Conditions: 20 mM Tris–HCl (pH 7.4), 150 mM KCl.

diagonal loop in this structure separates two pyrenes effectively, preventing from excimer formation and facilitating modest quenching of pyrene fluorescence by thymines present in the loop. On the other hand, fluorescence measurements in the presence of KCl revealed strong quenching that was attributed to the peculiarity of the potassium hybrid-type quadruplex, which enables effective stacking of pyrene moieties on the exposed guanine tetrads, thus facilitating static or electron transfer quenching. Stacking interactions with tetrad planes resulted in restriction of rotational freedom of pyrene tags, which was manifested by the substantial increase in fluorescence anisotropy with the increase in KCl concentration in contrast to the sodium quadruplex showing decrease in anisotropy with NaCl concentration. Plausibility of stacking interactions between pyrene and G-tetrad in a hybrid-type potassium quadruplex was further supported by the molecular modeling results.

All these valuable observations can be exploited for tuning the spectral performance of future fluorescent probes based on quadruplex formation. For systems that possess a basket-type quadruplex structure, a FRET approach is recommended (diminished stacking interactions). A chair-type quadruplex seems to be more suitable for the sensing approach that exploits stacking interactions between fluorophores, for example, excimer emission or contact quenching. Finally, for a hybrid-type quadruplex, which facilitates G-tetrad/fluorophore interactions, the approach with a single-labeled oligonucleotide with efficient hydrophobic fluorophore that is quenched by guanine can be recommended.

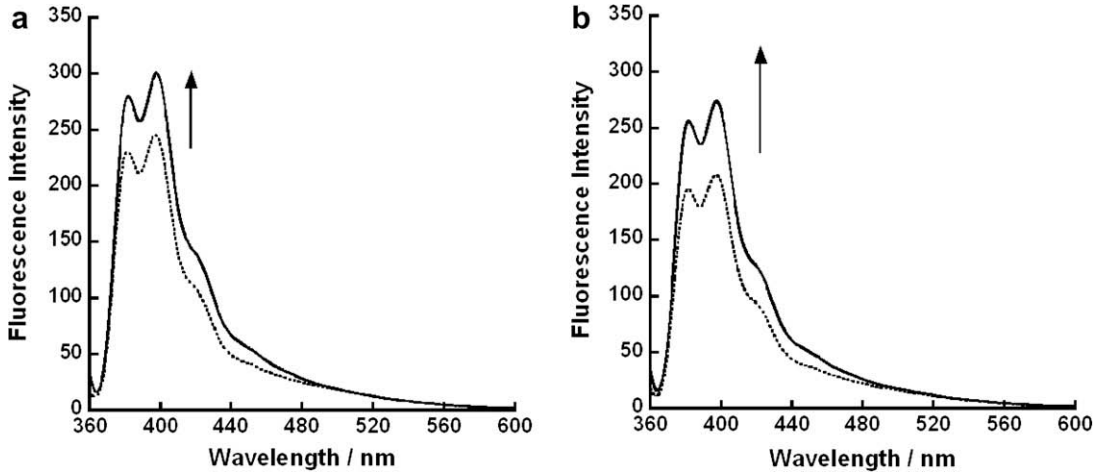

Figure 10. Fluorescence spectra of 0.2 μM Py-Htelom-Py(C3) (a), and 0. 2 μM Py-Htelom-Py(C6) (b) recorded in 50% PEG200 in the absence of salt (dashed line) and in the presence of 150 mM KCl (solid line). Conditions: 20 mM Tris–HCl (pH 7.4), λ_{ex} = 344 nm.

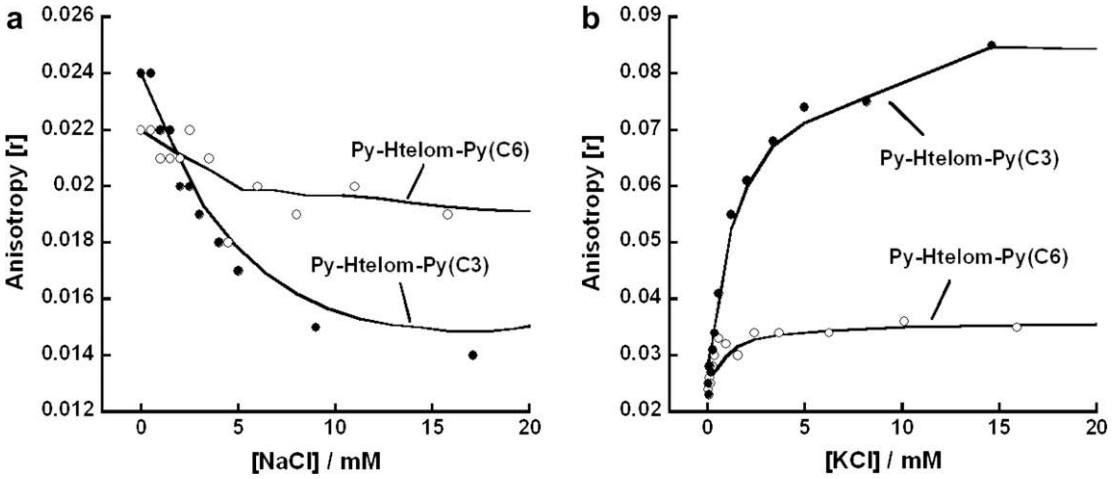

Figure 11. Anisotropy changes of Py-Htelom-Py(C3) and Py-Htelom-Py(C6) upon addition of NaCl (a) and KCl (b). Conditions: 20 mM Tris–HCl (pH 7.4), λ_{ex} = 344 nm.

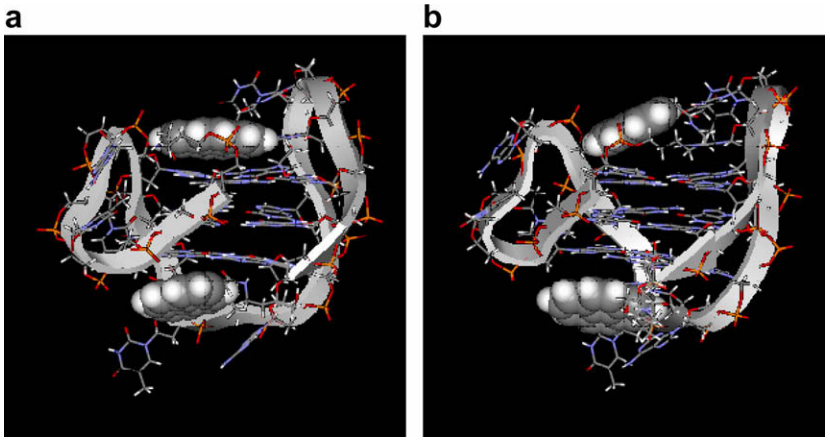

Figure 12. Optimized structures of the hybrid-type quadruplexes for Py-Htelom-Py(C3) (a), and Py-Htelom-Py(C6) (b) probes.

4. Experimental

4.1. Pyrene-labeled oligonucleotides

Pyrene-labeled oligonucleotides (Scheme 1) were custom-synthesized by Sigma-Genosys Japan (Ishikari, Japan) and purified by reversed phase HPLC and their identities were confirmed by MALDI-TOF MS (Voyager™). Stock solutions of the oligonucleotides were prepared in MilliQ water (Millipore, Billerica, MA). Other chemicals were of analytical grade.

4.2. CD spectra and melting experiments

Circular dichroism (CD) spectra and thermal denaturation experiments were recorded using a Jasco J-820 Spectropolarimeter (response, 100 mdeg; scan rate, 50 nm/min; response, 4 s; data collecting interval, 0.2 nm; band width, 2 nm; accumulated time, 4 times) at 25 °C.

Spectra were recorded at room temperature approximately 30 min after sample preparation in a 1 cm path length quartz cell using 2 μM solution of a probe in 20 mM Tris–HCl buffer (pH 7.4). Melting temperature (T_m) measurements were conducted in the following condition: response, 100 mdeg; temperature gradient, 30 °C/h; collecting wavelength, 292.6 nm; response, 8 s; data collecting interval, 0.5 °C; bandwidth, 2 nm. Both heating and cooling cycles were superimposed, indicating that melting process was kinetically reversible. Each experiment was performed in triplicate and mean values with standard deviations are reported. Thermodynamic parameters were calculated from the CD melting curves using a non-linear least squares fitting assuming a two-state equilibrium model and that heat capacity for folding is zero. These assumptions are commonly used[26] although they may not be strictly obeyed. Nevertheless calculated thermodynamic parameters can be compared with results reported by other authors.

4.3. Gel electrophoresis experiments

Non-denaturing gel electrophoresis experiments were performed with the Py-Htelom-Py probes and the unmodified Htelom oligonucleotide. Experiments were performed in a 20 mM Tris–HCl (pH 7.4) buffer containing 0.1 M KCl or 0.1 M NaCl. The samples were loaded onto a non-denaturing 20% polyacrylamide gel and run for 2 h (10 V/cm) at room temperature. The resulting gel was stained with GelStar and imaged with a digital camera.

4.4. Fluorescence spectra and anisotropy measurements

All fluorescence experiments were conducted with Perkin-Elmer LS-55 Luminescence Spectrometer (both slit widths of 10 nm) using a 10 mm quartz cell; the spectra were not corrected. Sample solution (600 μl) contained 0.2 μM of fluorescent oligonucleotide in 20 mM Tris–HCl buffer (pH 7.4). A typical titration consisted of successive additions of small portions (5 μl) of a concentrated solution of required salt, followed by stirring and thermal equilibration. Fluorescence probes were excited at 344 nm and the emission spectra were recorded in the 300–600 nm spectral range. All spectra were obtained on freshly prepared samples within 30 min of preparation. The cell compartment was thermostated at 25 °C and was equipped with a magnetic stirrer.

For anisotropy measurements, spectra were recorded using a set of polarizing filters. Anisotropy, r, was calculated from the following equation:

$$r = \frac{F_{VV} - F_{VH}G}{F_{VV} + 2F_{VH}G} \quad \text{with} \quad G = \frac{F_{HV}}{F_{HH}} \tag{1}$$

where F is integrated fluorescence, subscripts V and H represent vertical and horizontal setting of polarizers. The first index denotes excitation, the second-emission polarizer. G is used for instrumental correction.

References and notes

1. Kerwin, S. M. *Curr. Pharma. Des.* **2000**, *6*, 441.
2. Williamson, J. R. *Annu. Rev. Biophys. Biomol. Struct.* **1994**, *23*, 703.
3. Parkinson, G. N.; Lee, M. P.; Neidle, S. *Nature* **2002**, *417*, 876.
4. Haider, S. M.; Parkinson, G. N.; Neidle, S. *J. Mol. Biol.* **2003**, *326*, 117.
5. Blackburn, E. H. *Annu. Rev. Biochem.* **1984**, *53*, 163.
6. Macaya, R. F.; Schultze, P.; Smith, F. W.; Roe, J. A.; Feigon, J. *Proc. Natl Acad. Sci. U.S.A.* **1993**, *90*, 3745–3749.
7. Siddiqui-Jain, A.; Grand, C. L.; Bearss, D. J.; Hurley, L. H. *Proc. Natl. Acad. Sci. U.S.A.* **2002**, *99*, 11593.
8. Simonsson, T.; Pecinka, P.; Kubista, M. *Nucleic Acids Res.* **1998**, *26*, 1167.
9. Dai, J.; Chen, D.; Jones, R. A.; Hurley, L. H.; Yang, D. *Nucleic Acids Res.* **2006**, *34*, 5133.
10. Simonsson, T. *Biol. Chem.* **2001**, *382*, 621.
11. Davis, J. T. *Angew. Chem. Int. Ed.* **2004**, *43*, 668.
12. Neidle, S.; Parkinson, G. *Curr. Opin. Struct. Biol.* **2003**, *13*, 275.
13. Neidle, S.; Parkinson, G. *Nat. Rev. Drug Discovery* **2002**, *1*, 383.
14. Juskowiak, B.; Takenaka, S. *Methods Mol. Biol.* **2006**, *335*, 311.
15. Ueyama, H.; Takagi, M.; Takenaka, S. *J. Am. Chem. Soc.* **2002**, *124*, 14286.
16. Juskowiak, B.; Galezowska, E.; Zawadzka, A.; Gluszynska, A.; Takenaka, S. *Spectrochim. Acta A* **2006**, *64*, 835.
17. Nagatoishi, S.; Nojima, T.; Juskowiak, B.; Takenaka, S. *Angew. Chem. Int. Ed.* **2005**, *44*, 5067.
18. Nagatoishi, S.; Nojima, T.; Galezowska, E.; Gluszynska, A.; Juskowiak, B.; Takenaka, S. *Anal. Chim. Acta* **2007**, *581*, 125.
19. Wang, Y.; Patel, D. J. *Structure* **1993**, *1*, 263.
20. He, Y.; Neumann, R. D.; Panyutin, I. G. *Nucleic Acids Res.* **2004**, *32*, 5359.
21. Li, J.; Correia, J. J.; Wang, L.; Trent, J. O.; Chaires, J. B. *Nucleic Acids Res.* **2005**, *33*, 4649.
22. Luu, K. N.; Phan, A. T.; Kuryavyi, V.; Lacroix, L.; Patel, D. J. *J. Am. Chem. Soc.* **2006**, *128*, 9963.
23. Ambrus, A.; Chen, D.; Dai, J. X.; Bialis, T.; Jones, R. A.; Yang, D. Z. *Nucleic Acids Res.* **2006**, *34*, 2723.
24. Dai, J.; Punchihewa, C.; Ambrus, A.; Chen, D.; Jones, R. A.; Yang, D. Z. *Nucleic Acids Res.* **2007**, *35*, 2440.
25. Xu, Y.; Noguchi, Y.; Sugiyama, H. *Bioorg. Med. Chem.* **2006**, *14*, 5584.
26. Balagurumoorthy, P.; Brahmachari, S. K. *J. Biol. Chem.* **1994**, *269*, 21858.
27. Rujan, I. N.; Meleney, J. C.; Bolton, P. H. *Nucleic Acids Res.* **2005**, *33*, 2022.
28. Balagurumoorthy, P.; Brahmachari, S. K.; Mohanty, D.; Bansal, M.; Sasisekharan, V. *Nucleic Acids Res.* **1992**, *20*, 4061.
29. Phan, A. T.; Patel, D. J. *J. Am. Chem. Soc.* **2003**, *125*, 15021.
30. Pedroso, I. M.; Duarte, L. F.; Yanez, G.; Baker, A. M.; Fletcher, T. M. *Biochem. Biophys. Res. Commun.* **2007**, *358*, 298.
31. Wlodarczyk, A.; Grzybowski, P.; Patkowski, A.; Dobek, A. *J. Phys. Chem. B* **2005**, *109*, 3594.
32. Mergny, J.-M.; Maurizot, J-C. *ChemBioChem.* **2001**, *2*, 124.
33. Fujimoto, K.; Shimizu, H.; Inouye, M. *J. Org. Chem.* **2004**, *69*, 3271.
34. Winnik, F. M. *Chem. Rev.* **1993**, *93*, 587.
35. Hrdlicka, P. J.; Babu, B. R.; Sorensen, M. D.; Harrit, N.; Wengel, J. *J. Am. Chem. Soc.* **2005**, *127*, 13293.
36. Kawai, K.; Yoshida, H.; Takada, T.; Tojo, S.; Majima, T. *J. Phys. Chem. B* **2004**, *108*, 13547.
37. Langenegger, S. M.; Haener, R. *Chem. Commun.* **2004**, *24*, 2792.
38. Zhu, H.; Lewis, F. D. *Bioconjugate Chem.* **2007**, *18*, 1213.
39. Manoharan, M.; Tivel, K. L.; Zhao, M.; Nafisi, K.; Netzel, T. L. *J. Phys. Chem.* **1995**, *99*, 17461.
40. Vialas, C.; Pratviel, G.; Meunier, B. *Biochemistry* **2000**, *39*, 9514.
41. Miyoshi, D.; Nakao, A.; Toda, T.; Sugimoto, N. *FEBS Lett.* **2001**, *496*, 128.
42. Breslow, R. *Acc. Chem. Res.* **1991**, *24*, 159.